Two Phase Morphology Limits Lithium Diffusion in TiO₂ (Anatase): A ⁷Li MAS NMR Study

Marnix Wagemaker,[†] Roel van de Krol,[‡] Arno P. M. Kentgens,[§] Ad A. van Well,[†] and Fokko M. Mulder*,[†]

Contribution from the Interfaculty Reactor Institute, Delft University of Technology, Mekelweg 15, 2629 JB Delft, The Netherlands, Laboratory for Inorganic Chemistry, Faculty of Applied Sciences, Delft University of Technology, P.O. Box 5045, 2600 GA Delft, The Netherlands, and N. S. R. Center for Molecular Design, Synthesis and Structure, Department of Physical Chemistry/Solid-state NMR, University of Nijmegen, Toernooiveld 1, 6525 ED Nijmegen, The Netherlands.

Abstract: ⁷Li magic angle spinning solid-state nuclear magnetic resonance is applied to investigate the lithium local environment and lithium ion mobility in tetragonal anatase TiO₂ and orthorhombic lithium titanate Li$_{0.6}$TiO₂. Upon lithium insertion, an increasing fraction of the material changes its crystallographic structure from anatase TiO₂ to lithium titanate Li$_{0.6}$TiO₂. Phase separation occurs, and as a result, the Li-rich lithium titanate phase is coexisting with the Li-poor TiO₂ phase containing only small Li amounts ≈ 0.01. In both the anatase and the lithium titanate lattice, Li is found to be hopping over the available sites with activation energies of 0.2 and 0.09 eV, respectively. This leads to rapid microscopic diffusion rates at room temperature (D_{micr} = 4.7 × 10⁻¹² cm² s⁻¹ in anatase and D_{micr} = 1.3 × 10⁻¹¹ cm² s⁻¹ in lithium titanate). However, macroscopic intercalation data show activation energies of ∼ 0.5 eV and smaller diffusion coefficients. We suggest that the diffusion through the phase boundary is determining the activation energy of the overall diffusion and the overall diffusion rate itself. The chemical shift of lithium in anatase is independent of temperature up to ∼250 K but decreases at higher temperatures, reflecting a change in the 3d conduction electron densities. The Li mobility becomes prominent from this same temperature showing that such electronic effects possibly facilitate the mobility.

1. Introduction

TiO₂ (anatase) has been the subject of a large number of studies during the past decade. This interest arises from the possible application of TiO₂ in solar cells,[1−3] electrochromic devices,[4−7] and rechargeable lithium ion batteries.[8−11] The use of TiO₂ (anatase) as an electrode material in lithium ion batteries and electrochromic devices is based on its ability to accommodate charge in the form of small foreign ions, such as Li⁺ and H⁺ in an intercalation process.

Schematically, the electrochemical reaction can be written as TiO₂ + xLi⁺ + xe⁻ → Li$_x$TiO₂, where x is the mole fraction Li in TiO₂. The maximum Li insertion in TiO₂ (anatase) varies through the literature from x = 0.5 up to 1 depending on the temperature and experimental technique.[8,10−16] For chemical intercalation with *n*-butyllithium,[15] which has a potential of 1 V versus Li, x = 0.7 seems to be the most reliable value, while for electrochemical experiments x = 0.5 is most consistently reported for the maximum insertion ratio. The (elastic) interaction force between intercalated Li ions is attractive,[16] and weak Ti−Ti interactions are formed,[17] which result in phase separation. The repulsive Coulomb interaction between the lithium ions is expected to be responsible for the limitation of the lithium content to x = 0.7.[12,16]

TiO₂ (anatase) has a tetragonal phase (space group $I4_1/amd$, number 141). Cava et al.[12] determined the structure of the intercalation compound Li$_{0.5}$TiO₂ (lithium titanate) with neutron diffraction (space group *Imma*, number 74). The overall orthorhombic distortion of the atomic positions in the change from

* Corresponding author.
† Interfaculty Reactor Institute, Delft University of Technology.
‡ Laboratory for Inorganic Chemistry, Faculty of Applied Sciences, Delft University of Technology.
§ University of Nijmegen.
(1) Cao, F.; Oskam, G.; Searson, P. C.; Stipkala, J. M.; Heimer, T. A.; Farzad, F.; Meyer, G. J. *J. Phys. Chem.* **1995**, *99*, 11974−11980.
(2) Hagfeldt, A.; Grätzel, M. *Chem. Rev.* **1995**, *95*, 49−68.
(3) O'Regan, B.; Grätzel, M. *Nature* **1991**, *353*, 737−740.
(4) Bechinger, C.; Ferrere, S.; Zaban, A.; Sprague, J.; Gregg, B. A. *Nature* **1996**, *383*, 608−610.
(5) Cantão, M. P.; Cisneros, J. I.; Torresi, R. M. *Thin Solid Films* **1995**, *259*, 70−74.
(6) Ohzuku, T.; Hirai, T. *Electrochim. Acta* **1982**, *27*, 1263−1266.
(7) Ottaviani, M.; Panero, S.; Morzilli, S.; Scrosati, B. *Solid State Ionics* **1986**, *20*, 197−202.
(8) Bonino, F.; Busani, L.; Manstretta, M.; Rivolta, B.; Scrosati, B. *J. Power Sources* **1981**, *6*, 261−270.
(9) Huang, S. Y.; Kavan, L.; Exnar, I.; Grätzel, M. *J. Electrochem. Soc.* **1995**, *142*, L142.
(10) Ohzuku, T.; Takehara, Z.; Yoshizawa, S. *Electrochim. Acta* **1979**, *24*, 219−222.
(11) Ohzuku, T.; Kodama, T.; Hirai, T. *J. Power Sources* **1985**, *14*, 153−166.

(12) Cava, R. J.; Murphy, D. W.; Zahurak, S.; Santoro, A.; Roth, R. S. *J. Solid State Chem.* **1984**, *53*, 64−75.
(13) Kavan, L.; Grätzel, M.; Gilbert, S. E.; Klemenz, C.; Scheel, H. J. *J. Am. Chem. Soc.* **1996**, *118*, 6716−6723.
(14) Luca, V.; Hanley, T. L.; Roberts, N. K.; Howe, R. F. *Chem. Mater.* **1999**, *11*, 2089−2102.
(15) Wittingham, M. S.; Dines, M. B. *J. Electrochem. Soc.* **1977**, *124*, 1387−1388.
(16) Zachau-Christiansen, B.; West, K.; Jacobsen, T.; Atlung, S. *Solid State Ionics* **1988**, *28−30*, 1176−1182.
(17) Nuspl, G.; Yoshizawa, K.; Yamabe, T. *J. Mater. Chem.* **1997**, *7*, 2529−2536.

anatase to lithium titanate is small and leads to more regularly shaped TiO$_6$ octahedra in lithium titanate than in anatase. The change in symmetry is accompanied by a decrease of the unit cell along the *c*-axis and an increase along the *b*-axis, resulting in an increase of ~4% of the unit cell volume. In the lithium titanate phase, the Li ions are randomly located in half of the available interstitial octahedral 4e sites, which was also found in theoretical calculations.[18,19] Van de Krol et al.[20] have studied the structural changes during intercalation with in-situ X-ray diffraction (XRD). They reported that the phase transition accompanying the intercalation process is reversible and starts at insertion ratios larger than $x = 0.05$ for nanostructured TiO$_2$ (anatase) electrodes.[21] Electrochemically, the two phase system produced by the phase separation and transition results in a constant potential during insertion and extraction of Li for $0.05 < x < 0.5$.

The lithium ion diffusion in lithium titanate and in anatase is likely to occur along a diffusion path connecting the vacant octahedral (interstitial) sites.[19] The macroscopic diffusion coefficient obtained with chronoamperometry on CVD films was found to be 2×10^{-15} cm^2 s^{-1} for insertion and 6×10^{-15} cm^2 s^{-1} for extraction.[21] This is significantly smaller than those obtained for single crystalline anatase: 2×10^{-13} cm^2 s^{-1} for insertion and 6×10^{-13} cm^2 s^{-1} for extraction.[13] Activation energies for insertion and extraction were found to be 0.54 and 0.78 eV, respectively,[21] and 0.6 eV for diffusion.[18] These values are in good agreement with the calculated 0.5 eV activation energy for Li hopping from one interstitial site to another.[19,22]

Van de Krol et al.[23] suggested that the difference found between the rate of insertion and the rate of extraction may be due to a large difference between the Li$^+$ mobility in the coexisting phases TiO$_2$ (anatase) and Li$_{0.5}$TiO$_2$ (lithium titanate). Little is known concerning the microscopic lithium ion mobility in both phases. Therefore, the present investigation was initiated to study the lithium environment and mobility in Li-doped TiO$_2$ with an overall composition given by Li$_x$TiO$_2$, where x varies between 0.03 and 0.7. ^{7}Li solid-state MAS NMR is applied, because it can locally probe the chemical environment of Li via the chemical shift (resonance line positions) and quadrupolar interaction. The Li dynamics can be probed when Li hops from one site to another on a frequency comparable to, or shorter than, the relevant NMR spectral parameters expressed in frequency units.[24] Two main questions will be addressed: (i) in which crystallographic phase and with what concentration is the Li intercalated, and (ii) on what time scale and with what activation energy does the Li motion occur in each phase. Furthermore, the chemical shift may give information concerning the electronic local environment of Li. We mainly concentrate on the small insertion ratios where the ^{7}Li NMR signal is visible for the coexisting phases, anatase and lithium titanate. In contrast, at higher insertion ratios, $x > 0.2$, only the signal of lithium in lithium titanate is resolvable.[14] X-ray diffraction was employed to determine the relative amounts of anatase and lithium titanate, as well as to determine the domain size of each phase.

2. Experimental Section

2.1 Sample Preparation. Microcrystalline TiO$_2$ (anatase) (99%) was obtained from Janssen Chemica. X-ray diffraction showed the characteristic anatase structure. Li$_x$TiO$_2$ samples were prepared by chemical intercalation of the TiO$_2$ powder with *n*-butyllithium[15] (1.6 M, Aldrich). The TiO$_2$ powder was mixed with hexane (95+%, Aldrich), and the *n*-butyllithium was added while stirring the mixture. Six samples were prepared with different amounts of *n*-butyllithium to form Li$_x$TiO$_2$ with the overall compositions of $x = 0.03, 0.07, 0.12, 0.25, 0.5,$ and 0.7. All the lithium is intercalated within the TiO$_2$ powder, because *n*-butyllithium (with a potential of 1 V against lithium) reacts vigorously with TiO$_2$ anatase, as is illustrated by the direct change of color of the TiO$_2$ powder (white to blue) and the heat that develops during reaction. After 3 days with occasional stirring, the samples were filtered, washed with hexane, and dried. All sample preparations were carried out in an argon atmosphere glovebox to prevent reactions of Li with air. The darkness of the blue powder is visually proportional with the composition (deeper blue for large x). After preparation, the samples were subjected to wet chemical inductively coupled plasma spectroscopy (ICP) analysis to check the overall composition (ratio Li/Ti). These results confirmed that during preparation all the lithium reacts with the TiO$_2$ (anatase), thus yielding the overall compositions as mentioned. The sample preparation procedure was repeated several times with complete reproducibility.

2.2 X-ray Powder Diffraction. Structural characterization was performed using a Bruker D3 Advance X-ray diffractometer with Cu Kα radiation. A sample container with airtight Kapton foil windows filled with argon was used to prevent the samples from reacting with moisture or oxygen from air. To make sure the sample did not degrade during an experiment, the most intense lithium titanate peak was monitored before and after the measurement. By visual inspection, the sample remained blue for several months at least. The relative amounts of the two phases present in the samples, and the line widths, were determined by full Rietveld refinements.

2.3 Solid-State NMR Spectroscopy. ^{7}Li MAS NMR ($I = {}^3/_2$, 92.6% abundance) spectra were recorded on a Chemagnetics 400 Infinity ($B_0 = 9.4$ T) and a Chemagnetics 600 Infinity ($B_0 = 14.1$ T) operating at 155.4 and 233.2 MHz, respectively. The MAS probe head with 3.2 mm airtight zirconia rotors achieved spinning speeds up to 19.2 kHz in a dry nitrogen atmosphere. Chemical shifts were referenced to a 0.1 M LiCl aqueous solution. The spectra were recorded after a 30° (at $2\omega_{rf}$) radio frequency pulse applied with a recycle delay of 20 s. The 90° pulse length was 1.4 μs. The T_1 relaxation time was determined to be well below 5 s for all temperatures, using a saturation recovery experiment. Therefore, a pulse delay of 20 s was sufficient for quantitative measurements. Comparison of the integrated lithium signal intensity detected in lithium acetate and the Li$_x$TiO$_2$ samples indicated that all the lithium present in the samples was detected.

To observe the effect of degradation of the samples on the NMR spectra, samples were exposed to air intentionally. The spectra changed considerably for samples that were exposed to air for 1 h, while for 5 h of exposure the spectrum turned out to be completely degraded, yielding a spectrum similar to that of LiOH. Clearly, the samples are unstable in air, and LiOH is the most likely reaction product formed at the surface of the TiO$_2$. By visual inspection of the blue coloration, it appears that for low values of x the degradation proceeds more rapid than for high values of x. During the work presented here, the stability of the samples was monitored directly via the NMR spectra.

Two types of NMR experiments were performed yielding different types of information. (1) Structural information is obtained through the chemical shift using single pulse excitation MAS experiments for the different sample compositions. The influence of the temperature on the electronic local environment of Li is observed in terms of its influence on the chemical shift. (2) To explore the Li mobility, T_2 relaxation was measured under static, that is, nonspinning, conditions using a Hahn echo sequence ($\pi/2 - \tau - \pi - \tau - $ acq) for a range of temperatures (148−473 K). Thermally activated Li ion diffusion can

(18) Lunell, S.; Stashans, A.; Ojamae, L.; Lindstrom, H.; Hagfeldt, A. *J. Am. Chem. Soc.* **1997**, *119*, 7374−7380.

(19) Stashans, A.; Lunell, S.; Bergström, R.; Hagfeldt, A.; Lindquist, S. E. *Phys. Rev. B* **1996**, *53*, 159−170.

(20) Van De Krol, R.; Goossens, A.; Meulenkamp, E. A. *J. Electrochem. Soc.* **1999**, *146*, 3150−3154.

(21) Lindström, H.; Södergren, S.; Solbrand, A.; Rensmo, H.; Hjelm, J.; Hagfeldt, A.; Lindquist, S. E. *J. Phys. Chem. B* **1997**, *101*, 7710−7716.

(22) Koudriachova, M. V.; Harrison, N. M.; Leeuw, S. W. *Phys. Rev. Lett.* **2001**, *86*, 1275−1278.

(23) Van De Krol, R.; Goossens, A.; Schoonman, J. *J. Phys. Chem. B* **1999**, *103*, 7151−7159.

(24) Abragam, A. *Principles of Nuclear Magnetism*; Oxford Science Publications: Oxford, 1996.
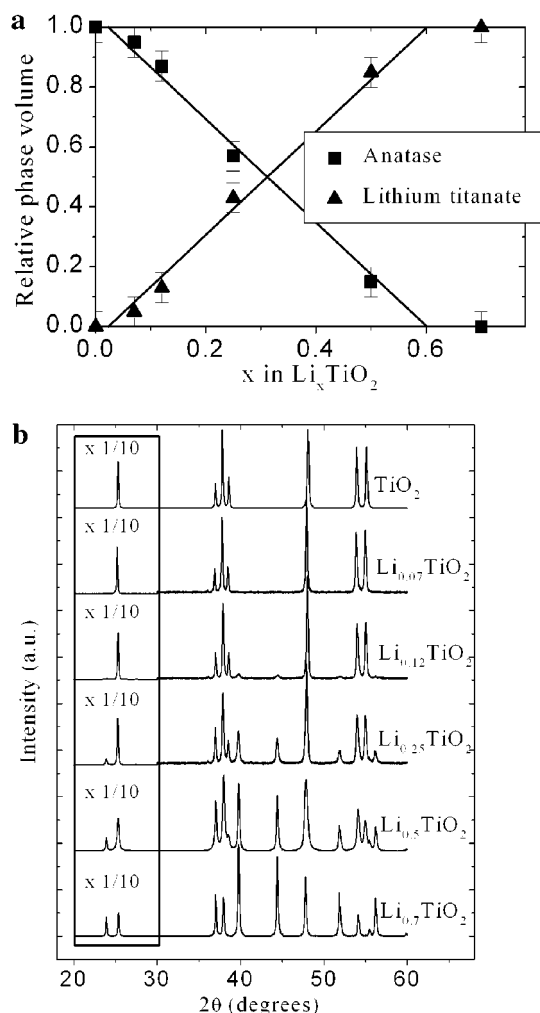
a

b

Figure 1. (a.) Phase fractions of anatase TiO_2 and lithium titanate versus inserted amount of Li, $x = Li/Ti$. (b.) X-ray diffraction spectra of lithium intercalated TiO_2 (anatase) for different overall compositions. The first parts of the spectra are scaled down to get a better view of the second parts.

increase the spin−spin relaxation time, T_2, with increasing temperature,[25] because of the averaging of interactions. The value of T_2, at the temperature just below the temperature at which T_2 starts to increase, is related to the lower limit of the average time a Li ion resides at one site before it hops to another site (correlation time)[25] at that temperature. For the present investigation, the T_2 relaxation under static conditions appeared to be more sensitive to Li diffusion than the T_2 relaxation under MAS conditions. The reason for this is that when the spinning speed is significantly larger than the dipolar interactions (both expressed in Hz) the spinning already averages dipolar interactions, leaving only relatively smaller effects of Li diffusion on the T_2 relaxation.

3. Lithium Distributions in Li_xTiO_2

3.1 XRD Results. The X-ray diffraction (XRD) patterns for the various amounts of lithium inserted in TiO_2 (anatase) are shown in Figure 1a. The powder pattern of the untreated sample is recognized as that of pure anatase (space group $I4_1/amd$, $a = 3.784$ Å, $c = 9.510$ Å).

The intercalation of lithium causes new reflections to occur in the XRD pattern, matching those reported in the literature for lithium titanate ($Li_{0.5}TiO_2$).[14,21,26,27] They are in agreement with the orthorhombic unit cell as determined by neutron diffraction (space group *Imma*, $a = 3.806$ Å, $b = 4.077$ Å, $c =$

(25) Slichter, C. P. *Principles of Magnetic Resonance*; Springer-Verlag: New York, 1992.

a

b

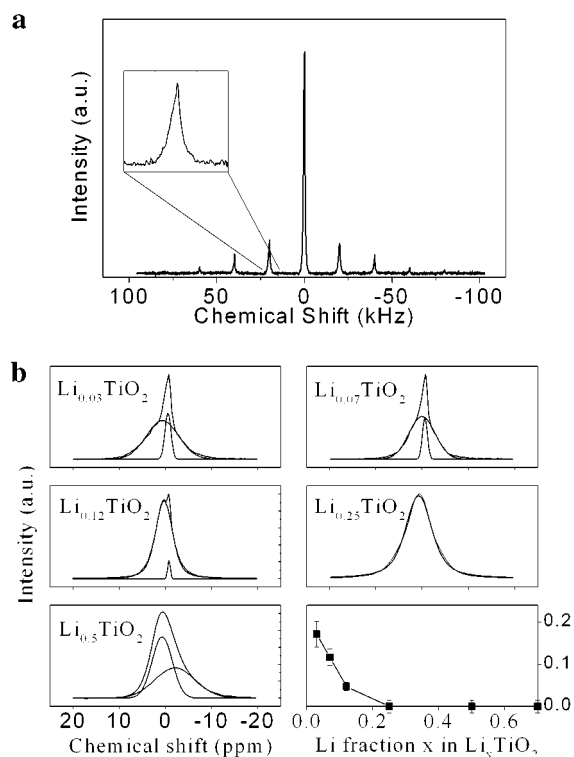**Figure 2.** (a.) Full ^7Li MAS NMR (Chemagnetics 400) spectrum for overall composition $Li_{0.12}TiO_2$; the inset of the first sideband illustrates that both species are present not only in the center band (Figure 2b). (b.) ^7Li MAS NMR (Chemagnetics 400) center band spectra at $T = 298$ K for different amounts of lithium intercalated, $x = Li/Ti$, in TiO_2 (anatase). The best fits are included; the spectral parameters of which are listed in Table 1. Bottom right-hand plot represents the relative ^7Li NMR peak area of Li in anatase (species C) versus x.

9.067 Å). For the compositions $x < 0.6$, both phases, anatase and lithium titanate, are present. At $x = 0.7$, all anatase has been totally phase transformed to the lithium titanate structure, illustrated by the absence of anatase reflections, see Figure 1b.

The presence of two phases may indicate that lithium is not homogeneously distributed over these two phases. The results are plotted versus the overall lithium content, x, in Figure 1b. The relative amount of each crystallographic phase is linearly proportional to the amount of inserted lithium, x. The Rietveld refinements showed line broadening of mainly the lithium titanate phase that may be attributed to a typical domain size of about 60−80 nm and limited internal strains. The unit cell of the anatase phase increases by only ∼0.3% upon lithium insertion, while lithium titanate has a 3.3% larger unit cell, more or less independent of the overall lithium content x.

3.2 ^7Li MAS NMR Results. The center bands of the ^7Li MAS NMR spectra for the various amounts of lithium inserted in anatase are displayed in Figure 2b. The full spectra are very similar for different x; therefore, only one is plotted in Figure 2a. Because fast MAS averages the dipolar interactions, the broad interaction probed by the sidebands originates either from quadrupole interactions or from chemical-shift anisotropy. The field independence of the static and MAS patterns expressed in hertz (not shown) indicates that it is due to first-order quadrupolar interactions. Spectral decomposition of the center band

(26) Murphy, D. W.; Greenblatt, M.; Zahurak, S. M.; Cava, R. J.; Waszczak, J. V.; Hull, G. W., Jr.; Hutton, R. S. *Rev. Chim. Miner.* **1982**, *19*, 441−449.

(27) Murphy, D. W.; Cava, R. J.; Zahurak, S. M.; Santoro, A. *Solid State Ionics* **1983**, *9−10*, 413−417.

Li Diffusion in TiO₂ (Anatase)

J. Am. Chem. Soc., Vol. 123, No. 46, 2001 11457

Table 1. ^{7}Li MAS NMR (Chemagnetics 400) Parameters at $T = $ 298 K for Lithium Intercalated in the Overall Composition Li_xTiO_2[a]

sample	species	δ (ppm)	fwhm (kHz)
$x = 0.03$	A	0.70 ± 0.1	0.85 ± 0.01
	C	-0.75 ± 0.05	0.15 ± 0.01
$x = 0.07$	A	0.60 ± 0.1	0.88 ± 0.01
	C	-0.86 ± 0.05	0.16 ± 0.01
$x = 0.12$	A	0.65 ± 0.1	0.99 ± 0.02
	C	-0.85 ± 0.07	0.11 ± 0.01
$x = 0.25$	A	0.69 ± 0.1	1.10 ± 0.02
$x = 0.50$	A	0.65 ± 0.1	1.00 ± 0.01
	B	-2.8 ± 0.3	1.61 ± 0.03

[a] Species A refers to Li in lithium titanate, and species C refers to Li in anatase.

reveals several contributions to the spectra that are listed in Table 1 (at high temperature, the different components are best visible, see also Figure 6). Accurate intensities of the contributions were obtained from fitting the RT line shapes of the resonance lines with a mix of a Gaussian and Lorentzian line shape, and keeping the shape constant for each of the samples, while fitting the relative intensities.

The samples with small Li/Ti ratios have a broad central resonance (species A) as well as a narrow resonance at about -0.8 ppm (species C). The contribution of the narrow resonance to the total spectrum decreases with increasing Li/Ti ratio, as illustrated in Figure 2b. Because the NMR measurements are performed quantitatively, the ratio between the integrated signal observed for both species equals the ratio of the amount of lithium in both environments. For these quantitative results, the whole spectra have been deconvoluted, including the sidebands. At the overall composition $x \geq 0.25$, species C is not visible anymore, and only species A remains. For $x = 0.5$ (and $x = 0.7$), a new resonance appears at -2.8 ppm (species B). The line shape of the spinning sidebands is much like the center band, although the narrow resonance, species C, is relatively weaker. The resonance referred to as "species A" and "species B" match the resonance observed by Luca et al.[14] They assigned species A as Li in the octahedral voids of the lithium titanate phase, and species B was suggested to be the result of a lithium species weakly coupled to conduction band electrons. The narrow resonance, species C, has not been observed before. This is not in contradiction with the results of Luca et al.[14] (who studied compositions $x \geq 0.3$), because species C only appears with measurable intensity at insertion ratios less than $x = 0.25$. Species A is the result of Li in lithium titanate; therefore, species C must be Li residing in another environment that gradually vanishes with increasing Li insertion, as is illustrated by Figure 2b. Therefore, species C has to be assigned to Li in anatase, the initial anatase TiO₂ phase that gradually disappears upon increased lithium insertion. We therefore confirm the thermodynamically stable two-phase system that was previously reported and also predicted by recently performed calculations.[22]

Combination of the X-ray and NMR data for the different overall compositions Li_xTiO_2 leads to a determination of the lithium fraction in the anatase and in the lithium titanate phase. Figure 1b gives the amount of both crystallographic phases from XRD, while in Figure 2b the fraction of lithium in the anatase phase is given. Combining these results, the composition of the anatase phase is $Li_x(TiO_2)$ with $x \approx 0.01$, and the composition of the lithium titanate phase is Li_xTiO_2 with $0.6 < x < 0.7$ for all the samples with overall Li composition $0.03 < x < 0.7$. The latter finding is in agreement with Murphy[27] and Wittingham.[15] Extrapolating the linear behavior in Figure 1b leads to $x \approx 0.6$ instead of $x = 0.5$ for the lithium rich phase (for the overall composition $Li_{0.5}TiO_2$, the original anatase phase is still

present, Figure 1a). Clearly, for increasing lithium concentration, there is a strong preference for the lithium titanate structure (composition $Li_{0.6-0.7}TiO_2$). The result indicates that the phase separation in anatase and lithium titanate takes place at even lower lithium concentrations than the suggested $x = 0.05$ by Van de Krol et al.[20]

Having assigned species C to lithium in anatase TiO₂, the chemical shift might lead to an indication of the oxygen coordination and, thus, to the position of lithium in the anatase lattice. On the basis of the resemblance of the anatase and lithium titanate structure, one might expect Li in anatase to reside in the octahedral voids. Lithium in lithium titanate is effectively 5-fold coordinated to oxygen (in the $a-b$ plane, two oxygens are at 1.97 Å and two at 2.04 Å, and in the c-direction, one is at 2.17 Å and one at 2.8 Å), while Li in the middle of the octahedral site in anatase is effectively 4-fold coordinated (four oxygens are in the $a-b$ plane at 1.93 Å and two in the c-direction at 2.78 Å). In the absence of other mechanisms influencing the chemical shift, 5-fold oxygen coordination would lead to a more positive chemical shift[28] for lithium in lithium titanate. This is indeed the case, as can be confirmed by inspecting Figure 2b, indicating that the Li may be in the octahedral voids.

Another feature of interest in the MAS spectra of Figure 2a is the presence of spinning sidebands. This broad spinning sideband manifold is a result of the interaction of the [7]Li quadrupole moment (-3×10^{-30} m²) with the electric field gradient. The quadrupole interaction (C_Q) is, next to the chemical shift, a second sensitive probe of the chemical environment of Li. The sidebands belong to both lithium in lithium titanate and in anatase. However, because the Li in anatase resonance is relatively weak, the width of its quadrupolar interaction is difficult to determine. On the basis of the positions of the ions surrounding Li and assuming point charges (i.e., an ionic charge model), an estimate for the quadrupole interaction constant, C_Q, and the asymmetry parameter, η, can be computed.[29] Using the position of Li in the lithium titanate[12] structure leads to $C_Q = 159$ kHz and $\eta = 0$, if the six nearest neighboring atoms are considered (all oxygen). This is in agreement with the width of the observed sideband manifold, which equals 160 kHz at $T = 298$ K (Figure 2a). For Li in the center of the anatase octahedral voids, one obtains $C_Q = 299$ kHz. On the basis of these values for C_Q, the second-order quadrupole broadening and the quadrupole induced shift can be calculated to be negligible in the presented measurements. The chemical shifts of both resonances can, therefore, be considered isotropic. The intensity of Li in anatase in the sidebands is, unfortunately, too weak to use to decide on the correctness of this value and, therefore, on the position of Li in the anatase lattice. The small concentration of Li in anatase complicates the experimental determination of the Li position in anatase by means of neutron diffraction, and to the best of our knowledge, it is not reported in the literature. However, the distorted octahedral voids are the most likely Li positions, because it is not in contradiction with the data and also in view of the position Li has in the very similar lithium titanate structure.

When examining the data, it appeared that there is a slight temperature dependence of the relative amounts of Li in the TiO₂ and lithium titanate phase. When fitted using a Boltzmann distribution, the Li in anatase could be viewed as being in an energy level $\sim$31 K above that of Li in lithium titanate. The

(28) Xu, Z.; Stebbins, J. F. *Solid State Nucl. Magn. Reson.* **1995**, *5*, 103.
(29) Koller, H.; Engelhardt, G.; Kentgens, A. P. M.; Sauer, J. *J. Phys. Chem.* **1994**, *98*, 1544−1551.
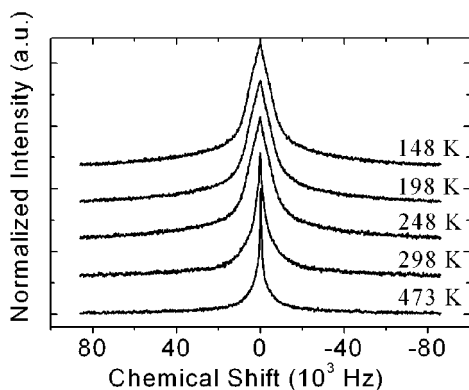
Figure 3. ^{7}Li static NMR (Chemagnetics 600) spectra for overall composition $Li_{0.12}TiO_2$ obtained with a Hahn echo pulse sequence for a number of temperatures illustrating the effect of Li diffusion on the line width (motional narrowing).

small change in the relative amounts of Li in both phases shows that there is exchange of Li on prolonged time scales between the two phases. This is a matter of further investigation and falls outside the scope of this paper.

4. Lithium Mobility

4.1 Static and MAS ^{7}Li NMR Results. In the remainder, we concentrate on the sample with overall composition $Li_{0.12}TiO_2$ where species A and C are both measurable, i.e., $x < 0.25$. The static ^{7}Li spectra for overall composition $Li_{0.12}TiO_2$ at different temperatures are displayed in Figure 3. The broad, ~160 kHz, wings in the spectra stem from the powder pattern of the $\pm^{1}/_{2} \leftrightarrow \pm^{3}/_{2}$ satellite (nuclear spin) transitions, which are separated from the central transition because of the quadrupole interactions described previously. The central peaks in Figure 3 can be decomposed into two more narrow components resulting from the $-^{1}/_{2} \leftrightarrow +^{1}/_{2}$ central transition of, respectively, Li in lithium titanate (~12 kHz below 198 K) and Li in anatase (~1.3 kHz below 198 K). These two central transitions of Li in both phases display strong line narrowing with increasing temperature above 198 K. This is attributed to motional narrowing as a result of increased lithium mobility in the lattice.

Motional narrowing occurs when the lithium hopping frequency between sites exceeds a relevant nuclear hyperfine interaction (expressed in hertz), ultimately leading to effective averaging of the interaction. The possible relevant interactions of ^{7}Li with its environment are (1) the magnetic dipolar coupling and (2) the quadrupolar interaction. Both are discussed in more detail with respect to mobility in the following.

(1) Given the largest nuclear spins of Ti (^{49}Ti, $-1.1039 \mu_N$, 5.5% natural abundance (n.a.); ^{47}Ti, $-0.7883 \mu_N$, 7.5% n.a.), O (0.0 μ_N), and Li (^{7}Li, 3.256 μ_N, 92.5% n.a.; ^{6}Li, 0.822 μ_N, 7.5% n.a.), the nuclear dipolar interaction in polycrystalline anatase and lithium titanate can be estimated.[24] The dipolar coupling in lithium titanate will be dominated by the Li−Li interactions on the shortest possible Li−Li distances (2.54 Å),[12] while for the low density of Li in anatase the dipolar interaction will be dominated by the shortest Ti−Li distances (2.676 Å). The lattice sum of all the dipolar interactions leads for lithium titanate to a static (or rigid lattice) powder line width of ~8 kHz and leads for anatase to ~1.0 kHz, assuming that for both phases Li resides in the center of the oxygen octahedra. For both species, the calculated value is smaller but in fair agreement with the line width observed in the decomposition of the central peak in the low temperature spectra (Table 2). It is worth mentioning that

Table 2. Spectral Decomposition of the ^{7}Li Static NMR (Chemagnetics 400) Central Transition for a Range of Temperatures[a]

temperature	species	δ (ppm)	fwhm (kHz)
$T = 148$ K	A	0.59 ± 0.15	11.8 ± 0.2
	C	-0.73 ± 0.1	1.35 ± 0.07
$T = 198$ K	A	0.60 ± 0.16	11.8 ± 0.2
	C	-0.70 ± 0.1	1.35 ± 0.1
$T = 248$ K	A	0.65 ± 0.15	11.7 ± 0.2
	C	-0.67 ± 0.08	1.12 ± 0.06
$T = 298$ K	A	0.61 ± 0.13	11.2 ± 0.2
	C	-0.80 ± 0.07	0.89 ± 0.04
$T = 398$ K	A	0.55 ± 0.11	6.94 ± 0.15
	C	-1.4 ± 0.07	0.63 ± 0.05

[a] Overall sample composition $Li_{0.12}TiO_2$; species A refers to Li in lithium titanate, and species C refers to Li in anatase.

the difference in NMR line width between species A and C can now be explained from the difference in Li density between Li in anatase (species C) and Li in lithium titanate (species A). Li diffusion can average the dipolar interaction to zero, provided that Li hopping rates are fast compared to the dipolar interactions[25] in lithium titanate and anatase, respectively.

(2) The symmetry of the octahedral voids in both lithium titanate and anatase is such that the different sites have opposite orientation of the quadrupole tensor with respect to the applied field but no difference in absolute value. As a result, the quadrupolar interaction may be averaged within one powder particle, assuming it is a single crystal, leading to a collapse of the spectrum toward the central line. The quadrupolar interactions of more than 100 kHz are larger than the dipolar interactions. This implies that the dipolar interactions should start to be averaged by motions at lower temperatures than those of the quadrupolar interactions. The present results do not show significant change in the width of the quadrupole spectrum with temperature. Therefore, the Li mobility was not high enough to cause a significant collapse in the MAS spectra and the disappearance of the spinning sidebands. It may also be noted that for the relatively small quadrupolar interaction the second-order quadrupolar interaction is negligible compared to the line widths observed.

In view of the considerations described here, Figure 3 indicates the averaging of the nuclear dipolar interactions of Li in both the anatase and lithium titanate environment, clearly evidencing temperature dependent Li mobility in both phases. It should be noted here that the dipolar interactions can only be averaged significantly when the positions of Li nuclei relative to all other nuclei sample many different positions with sufficiently fast rates. Some more local Li motion, for example, inside the octahedral sites, is not enough to yield the strong motional narrowing effects as observed, because the average position relative to the other nuclei does not change significantly, and with it, the dipolar relaxation does not change much. In fact, local motions, if present, may be expected on more rapid time scales than those probed with T_2; that is, they may be visible in a temperature dependence of T_1. Because the latter is almost absent in both phases, this indicates that there is no relevant Li (local) motion on time scales close to the Larmor frequency (~10^7−10^9 Hz). We also have to conclude that the change observed in T_2 is due to Li hopping between different interstitial sites.

An often-applied model for the spin−spin relaxation due to fluctuations in the dipolar interactions caused by diffusion is the Bloembergen, Purcell, and Pound (BPP) model.[30] An

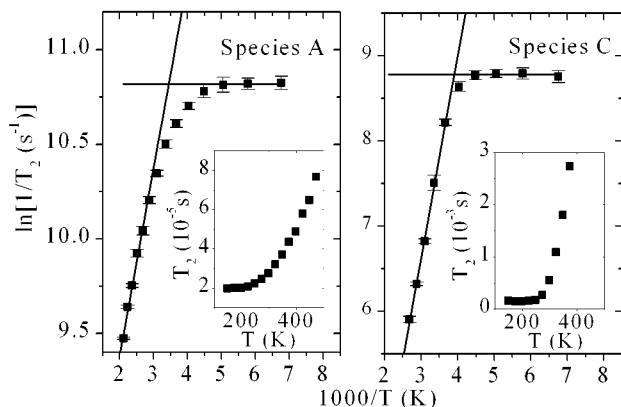(30) Bloembergen, N.; Purcell, E. M.; Pound, R. V. *Phys. Rev.* **1948**, *73*, 679.

Figure 4. Arrhenius plot of the ^{7}Li spin−spin relaxation time T_2 for the coexisting phases with the overall sample composition $Li_{x=0.12}TiO_2$ (species A, Li in lithium titanate; species C, Li in anatase). Data were acquired under nonspinning conditions (Chemagnetics 600). The lines cross at a temperature where the T_2 can directly be related to correlation time of Li motion. The insets give the same results plotted as T_2 versus temperature.

example for the determination of diffusion coefficients using the BPP model for T_2 relaxation, and comparing them with macroscopic data, is Holcomb et al.[31] for the alkali metals Na and Li. In the following, the BPP model will be applied.

4.2 Mobility from T_2 Spin−Spin Relaxation. Now that we know the origin of the line narrowing, a quantitative analysis of the motion can be performed by analyzing the spin−spin relaxation times as a function of temperature. The static T_2 spin−spin relaxation time for each of the phases is shown in Figure 4, at temperatures ranging from 148 to 473 K. For both species, T_2 does not vary until a certain temperature, while for higher temperatures a significant increase is observed.

In case of identical nuclei, the BPP model for T_2 relaxation yields

$$1/T_2 = C_{dipole}\left\{ \frac{3}{2}\tau_c + \frac{5}{2}\frac{\tau_c}{(1+\omega_0^2\tau_c^2)} + \frac{\tau_c}{(1+4\omega_0^2\tau_c^2)} \right\}$$

where C_{dipole} is proportional to the rigid lattice second moment $\langle\Delta\omega^2\rangle$. τ_c is the correlation time defining the time between Li hops, and ω_0 is the Larmor frequency. The expression for $1/T_2$ holds only for rapid motion, that is, $\langle\Delta\omega^2\rangle^{1/2}\tau_c \ll 1$; for slow motion, that is, $\langle\Delta\omega^2\rangle^{1/2}\tau_c \gg 1$, $1/T_2$ equals the static line width $\langle\Delta\omega^2\rangle^{1/2}$. Between the two regimes, a break point occurs where $\tau_c = T_2/\sqrt{2}$. If we assume the mobility of the ions to be thermally activated, the correlation time will obey an Arrhenius law, $\tau_c = \tau_\infty \exp(E_A/k_BT)$, where E_A is the activation energy of the jump process, and $1/\tau_\infty$ is the attempt frequency. For large T_2, the correlation times obey $\langle\Delta\omega^2\rangle^{1/2}\tau_c \ll 1$, but still $\omega_0\tau_c \gg 1$, which means that, within the BBP model,

$$1/T_2 = 3\tau_c C_{dipole}/2 \propto \tau_\infty \exp(E_A/k_BT)$$

Therefore, an Arrhenius plot of $\ln(1/T_2)$ versus $1/T$ in this range leads to a determination of the activation energy. Figure 4 gives the Arrhenius plot for both phases. The linear fit results in activation energies of $E_A = 0.20 \pm 0.01$ eV (2400 K) and $E_A = 0.09 \pm 0.01$ eV (1000 K) for Li in anatase and lithium titanate, respectively. The break point between the low and high mobility regime indicated by the crossing lines in Figure 4 leads via $\tau_c = T_2/\sqrt{2}$ to approximate values for the correlation time, 0.17 ms at ~250 K for anatase and 0.019 ms at ~290 K for

(31) Holcomb, D. F.; Norberg, R. E. *Phys. Rev.* **1955**, 98, 1074

lithium titanate. With these values, τ_∞ is computed to be 16 ns for Li in anatase and 620 ns for Li in lithium titanate. At room temperature, this leads to $\tau_c = 47$ μs for anatase and 17 μs for lithium titanate.

An estimate of the microscopic diffusion coefficient D at room temperature can be determined with $D = l^2/n\tau_c$, where l is the length of an elementary jump between sites, and n the number of possible jumps leading to different nearest neighbor sites. In both phases, lithium can be expected to hop from the octahedral interstitial sites to four other equivalent sites ($n = 4$) at a distance 2.96 Å for anatase and 3.03 Å[19] for lithium titanate, resulting at room temperature in $D_{micr} = 4.7 \times 10^{-12}$ cm^2 s^{-1} and $D_{micr} = 1.3 \times 10^{-11}$ cm^2 s^{-1}, respectively.

The dependence on overall Li content was checked by performing similar experiments as described previously for $Li_{0.12}TiO_2$ for the overall composition of $Li_{0.07}TiO_2$. This resulted in the same results for Li mobility in both phases.

4.3 Discussion. The estimated values for the microscopic diffusion coefficients in both phases are considerably larger than several reported in the literature for electron beam evaporated[23] and CVD[21] films ($\approx 10^{-15}$ cm^2 s^{-1}) for the overall diffusion coefficient of Li in TiO$_2$ as determined with electrochemical techniques. Furthermore, the activation energy for Li hopping is in both anatase and lithium titanate considerably smaller than values determined electrochemically via the temperature dependence of the diffusion coefficient: $E_A = 0.54$ and 0.78 eV[21] (insertion and extraction) and 0.6 eV.[18]

The main difference between electrochemical methods and NMR that may explain the differences in diffusion constants is that NMR probes diffusion rates on a scale of nanometers. Therefore, Li diffusion observed by NMR is not affected by surface effects, grain boundaries, or crystallographic phase boundaries. In principle, these types of diffusion need not have the same activation energy, and they all may be overall diffusion limiting processes in a macroscopic electrochemical diffusion measurement. In fact, one of these processes has to limit the electrochemically determined diffusion coefficient, because the diffusion within each phase is higher and has lower activation energy.

For macroscopic Li intercalation in TiO$_2$, the bulk diffusion is considered to be rate limiting,[23] which eliminates surface effects (contact with the electrolyte) to dominate the overall diffusion. The effect of grain boundaries between different crystallites can be illustrated by a study on Li insertion in single crystal TiO$_2$ (anatase) that reported electrochemically determined diffusion coefficients of, respectively, 2×10^{-13} and 6×10^{-13} cm^2 s^{-1} for Li insertion and extraction.[13] Compared to the $D \approx 10^{-15}$ cm^2 s^{-1} on polycrystalline materials, these values are relatively closer to the present observation ($D_{micr} = 4.7 \times 10^{-12}$ cm^2 s^{-1} and $D_{micr} = 1.3 \times 10^{-11}$ cm^2 s^{-1}). Note that one can actually not speak of single crystalline anatase, because Li insertion is accompanied with the phase transition from anatase ($Li_{0.01}TiO_2$) toward lithium titanate ($Li_{0.6}TiO_2$), resulting in the two coexisting phases. The "single crystal" values for the diffusion coefficient (2×10^{-13} and 6×10^{-13} cm^2 s^{-1})[13] thus include the phase boundary dynamics and the diffusion of Li through this crystallographic phase boundary. The "single crystal" result for the diffusion coefficient is still more than 1 order of magnitude smaller than the present results for within each phase. Assuming the experimental observations at the macroscopic level[18,21] and at the microscopic level (the present investigation) are correct, the macroscopic activated behavior with $E_A \approx 0.5$ eV cannot be due to Li inside each of the two phases, for the simple reason that Li has a lower E_A in both
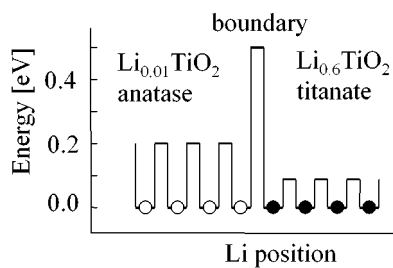
Figure 5. Schematic view of the energy barriers for Li motion in the anatase and lithium titanate two-phase system constructed from the microscopic activation energies in combination with macroscopic Li transport measurements.

phases (0.2 and 0.09 eV, respectively). This leads to the proposition that the microscopic diffusion within the phases is not rate limiting, but the Li diffusion between phases (or the movement of the phase boundary) must be overall diffusion rate limiting.

The energy barriers encountered by a single Li ion in the two-phase system resulting from the previous discussion are sketched in Figure 5. The bottoms of the potential wells in anatase and lithium titanate differ by only 31 K ($\sim$3 meV). Li moving through this system will encounter different barriers. Upon Li insertion from the right, the Li will have to cross the large 0.5 eV barrier (approximate value found in macroscopic measurements), while for extraction toward the right, only smaller 0.09 eV barriers are encountered. The overall diffusion would be limited by the largest barrier, which is formed by the phase boundary. In principle, such a model could explain that there is a smaller overall diffusion coefficient for insertion than for extraction of Li.

5. Electronic Structure

5.1 Temperature Dependence of the Chemical Shift. In Figure 6a,b, the chemical shift (CS) variations of Li in anatase (species C) and of Li in lithium titanate (species A) versus temperature are plotted for overall composition $Li_{0.12}TiO_2$. Similar results were obtained for overall composition $Li_{0.07}TiO_2$ (not shown). The chemical shift of Li in anatase is constant for $T = 173-273$ K, while it decreases approximately linearly for $T = 298-473$ K. The chemical shift of Li in lithium titanate (species A) seems to display the same behavior, although less prominently. As a result of the larger line width of species A, compared to that of species C, its chemical shift values are less accurate.

The decrease of the CS with temperature indicates a reduction in the field measured at the Li nucleus. The structure at these temperatures is not expected to change, and thermal expansion has a different temperature dependence than that observed for the CS. Thus, the observed shift is most likely the result of interactions of the Li nucleus with (conduction) electrons. There are two mechanisms to consider. First, paramagnetic interaction with unpaired localized electrons can influence the CS. Second, the Li nucleus may interact with conduction electrons (Knight shift).

5.2 Discussion. In principle, TiO_2 anatase is a large gap semiconductor with band gap $\sim$3 eV. Upon $Li^+ + e^-$ insertion, the electron may become localized on Ti or it may be inserted in a conduction band. If the electron becomes localized on Ti^{3+}, the atom might have a paramagnetic moment (if it is not quenched), while Ti^{4+} is nonmagnetic. Paramagnetic ions lead through Fermi contact interactions and the through space dipolar interaction to a paramagnetic induced shift which has a Curie–
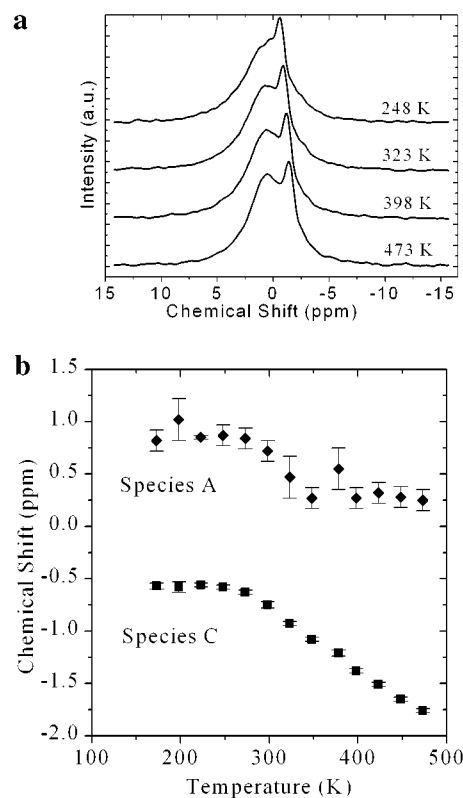

Figure 6. (a) ^{7}Li MAS center band for overall sample composition $Li_{0.12}TiO_2$ for different temperatures illustrating the temperature dependence of the chemical shift. (b) Temperature dependence of the ^{7}Li MAS chemical shift in anatase (species C) and lithium titanate (species A) for the overall sample composition $Li_{0.12}TiO_2$.

Weiss $1/T$ temperature dependence. The small variation with temperature of the CS of Li in TiO_2 starting at $\sim$250 K in Figure 6b cannot be described with such temperature dependence. Another argument for the absence of paramagnetic Ti^{3+} is the value of the T_1 relaxation parameter in these materials, which is well above 1 s. In materials with paramagnetic ions, T_1 is lowered significantly, even for very low concentrations, and can become as low as 10^{-4} s. The presence of localized electron states leading to paramagnetic Ti^{3+} is, thus, unlikely. This is also in agreement with magnetic susceptibility and EPR results of Luca et al.,[14] indicating that the Ti^{3+} density has to be very small.

Because there appears no room to interpret the results in terms of localized electron states, one should expect a more delocalized electron density. It is known that for pure anatase TiO_2 above 150 K there is a contribution to the magnetic susceptibility from the conduction band electrons.[32] These conduction electrons have, in principle, a temperature independent Pauli paramagnetism. However, the occupation of the conduction band in a semiconductor like anatase TiO_2 and low Li concentration doped anatase $Li_{0.01}TiO_2$ depends on temperature, which leads to intrinsic temperature dependence. The contribution of the conduction electron density to the chemical shift, referred to as the Knight shift K, is, thus, in principle, dependent on temperature. The basic equation for K is

$$K = \frac{\Delta\omega}{\omega} = \frac{8\pi}{3}\chi_e\langle|u(0)|^2\rangle_{\epsilon_F}$$

where χ_e is the Pauli susceptibility of the conduction electrons,

(32) Chauvet, O.; Forro, L.; Kos, I.; Miljak, M. *Solid State Commun.* **1995**, *93*, 667−669.

and $\langle|u(0)|^2\rangle_{\epsilon_F}$ represents the electron density with energy close to the Fermi level ϵ_F as measured at the Li nucleus.

In Li intercalated TiO_2 (anatase), the conduction band is mainly build out of 3d orbitals,[19,33] as is also more generally the case for transition metal oxides.[34] Because Li has O as nearest neighbors, the effect of 3d electron densities on the electron densities at ^7Li and the CS must therefore be transferred via O electronic states toward the Li atom. It is known that there can be a slight admixture of the O 2p states in the conduction band in lithium titanium oxides,[33] which would mean that increasing conduction electron densities would slightly increase the O 2p occupations. Such an increase in O 2p density appears to reduce the occupation of Li 2s states (by "core polarization"), resulting in a lowering of K with increasing temperature. The temperature dependence of the ^7Li CS in anatase and in lithium titanate (lower CS with higher T) may therefore indicate an increase of the delocalized Ti 3d and O 2p electron density with temperature. The potential of lithium intercalation is sensitive to the admixture of O 2p states in the conduction band,[35] indicating that these states are also important for the potential landscape encountered by Li.

Concerning the interaction with conduction electrons, it is also interesting that Luca et al.[14] concluded that the negative shift of resonance B (only detected for overall composition $x > 0.3$) was due to a weak coupling of the Li nucleus to conduction band electrons. Luca et al. did not detect any temperature dependence for species A and B for 200−300 K. This is not in contradiction with the present results, because the temperature dependence starts above 250 K and the effect is rather small for species A.

At the same temperature that the chemical shift starts to be temperature dependent, the lithium appears to be mobile in both anatase and lithium titanate. This may suggest that the activation energy for Li motion is influenced by excitations in the electronic environment. A mechanism for that would include the enhanced electronic screening of the ionic charges surrounding Li by conduction electrons. On the basis of quantum chemical calculations, Lunell et al.[18] suggested a coupling between electron and a diffusing ion in such a way that the charge-compensating electron occupies the 3d states of the nearest neighboring Ti atoms and effectively follows the lithium ion when it diffuses. This is corroborated by the present interpretation of the temperature dependent CS in the following way. With increasing temperature, the Ti 3d, O 2p conduction band occupation is increasing, while core polarization of the Li 2s states decreases the electron density measured directly at the Li nucleus. This would explain the observed small decrease

of the ^7Li CS. Thus, the small variation in the electron density measured at the Li nucleus indicates that the conduction electrons extend over some distance. The time scales of the Li ion hopping (slow) and the electronic mobility (fast) will be very different, which would imply that effectively this delocalized electron cloud is surrounding the Li ion on its way. Possibly, this influences the potential landscape in such a way that it facilitates the Li mobility.

6. Conclusions

The NMR results allow the assignment of two coexisting lithium containing crystallographic phases in TiO_2 (anatase), a Li-rich (lithium titanate) and a Li-poor phase (anatase). The combination of X-ray and NMR data for the different overall compositions of Li_xTiO_2 leads to a Li fraction in the Li-poor anatase phase of $x \approx 0.01$ and of $0.6 < x < 0.7$ in the Li-rich lithium titanate phase for all samples investigated. Apparently, TiO_2 (anatase) allows only a small Li fraction ($x \approx 0.01$) in the tetragonal structure before the Li imposes the phase transition toward the orthorhombic lithium titanate structure.

Motional narrowing and the large variation of the spin−spin T_2 relaxation times prove the lithium in both phases to be mobile at room temperature on a time scale in the order of 47 μs in anatase and 17 μs in the lithium titanate. The Arrhenius behavior of T_2 versus temperature indicates activated Li hopping with activation energy values of 0.2 eV in the Li-poor anatase and 0.09 eV in the Li-rich lithium titanate. The room temperature microscopic diffusion coefficients in the anatase and in the lithium titanate phase are 4.7×10^{-12} cm² s⁻¹ and 1.3×10^{-11} cm² s⁻¹, respectively. The difference between the results obtained here for the microscopic diffusion and the overall macroscopic diffusion determined by others suggests that the lithium diffusion through, or the dynamics of, the phase boundaries in this two phase system limits the overall diffusion and also dictates the overall activation energy.

The chemical shifts of lithium in anatase and in lithium titanate are independent of temperature up to about 250 K and decrease at higher temperatures, indicating a change in mainly the 3d conduction electron density. The change becomes observable at the same temperature as that at which the motion of Li appears, suggesting that the electronic structure influences the Li mobility.

(33) Benco, L.; Barras, J.-L.; Daul, C. A. *Inorg. Chem.* **1999**, *38*, 20−28.

(34) Bruce, P. G. *Solid State Electrochemistry*; Cambridge University Press: New York, 1995.

(35) Benco, L.; Barras, J.-L.; Atanasov, M.; Daul, C. A.; Deiss, E. *Solid State Ionics* **1998**, *112*, 255−259.